

Journal of Materials Chemistry B

Accepted Manuscript



This is an *Accepted Manuscript*, which has been through the Royal Society of Chemistry peer review process and has been accepted for publication.

Accepted Manuscripts are published online shortly after acceptance, before technical editing, formatting and proof reading. Using this free service, authors can make their results available to the community, in citable form, before we publish the edited article. We will replace this *Accepted Manuscript* with the edited and formatted *Advance Article* as soon as it is available.

You can find more information about *Accepted Manuscripts* in the [Information for Authors](#).

Please note that technical editing may introduce minor changes to the text and/or graphics, which may alter content. The journal's standard [Terms & Conditions](#) and the [Ethical guidelines](#) still apply. In no event shall the Royal Society of Chemistry be held responsible for any errors or omissions in this *Accepted Manuscript* or any consequences arising from the use of any information it contains.

Rational Design and Fabrication of Cancer-targeted Chitosan Nanocarrier to Enhance Selective Cellular Uptake and Anticancer Efficacy of Selenocystine

Cite this: DOI: 10.1039/x0xx00000x

Received 00th January 2014,
Accepted 00th January 2014

DOI: 10.1039/x0xx00000x

www.rsc.org/

Bo Yu [#], Hong Li [#], Jinhui Zhang, Wenjie Zheng and Tianfeng Chen*

Rational design and fabrication of nano delivery systems to encapsulate drugs, has been proven to be a promising and effective strategy for cancer therapy. Selenocystine (SeC), a naturally occurring selenoamino acid, has received more and more attention due to its novel pharmacological properties in treatments of cancers. In this study, we fabricated a cancer-targeted nanodrug delivery system by encapsulating SeC into chitosan (CS) nanoparticles with folate surface decoration (FA-SeC-CSNPs), and evaluated its antiproliferative activities. The nanosystem entered the cells through endocytosis and released SeC in lysosome under acidic environment. Compared with SeC-CSNPs and SeC, FA-SeC-CSNPs significantly inhibited the growth of HeLa human cervical cancer cells that overexpressed folate receptor through induction of apoptosis, with the involvement of PARP cleavage and caspase activation. Moreover, FA-SeC-CSNPs also significantly suppressed the migration and invasion of HeLa cells in a dose-dependent manner. Furthermore, the intracellular nanosystem triggered reactive oxygen species (ROS) overproduction as early as 25 min after treatment, which activated various downstream signaling pathways such as p53, AKT and MAPKs, to induce the cell death. Taken together, this study demonstrate a strategy for rational design of cancer-targeted nanosystem loading selenocompounds to achieve selective cellular uptake and enhanced anticancer efficacy.

1 Introduction

Nanotechnology has gained increasingly intensive attention due to its broad applications in medicine, biomaterials, electronics and energy production¹. Doxorubicin (Dox) liposomal, doxorubicin encapsulated in a stealth liposome, is one of the famous applications of nanotechnology in clinical cancer therapy and is now widely used to treat AIDS-related Kaposi's sarcoma, breast cancer, ovarian cancer and other solid tumors^{2,3}. In recent times, the advances in the field of nanotechnology and tumor biological technology has brought nanodrug delivery system to develop novel drugs that demonstrate increasing applications in cancer-targeted therapy⁴. Targeting modification could enhance the recognition and internalization of nanodrug delivery system by cancer cells, thus reduce the administrated dosage and undesirable toxic side effects⁵. Folic acid (FA) is a ligand that is useful for targeting cell membrane and enhancing nanoparticle endocytosis via the folate receptor^{6,7}. It is a stable, inexpensive, and generally poorly immunogenic chemical with a high affinity for the folate receptor.

Natural products have proven to be the most reliable single source of new and effective nano fabrication agents^{8,9}.

Chitosan (CS), the deacetylated form of the polysaccharide chitin (a byproduct of crustaceans), is blind to negatively charged lipids in animal trials¹⁰. Owing to its special properties, including non-toxicity, novel antimicrobial activity, high biodegradability and biocompatibility, CS is receiving increasing attention in the pharmaceutical field for a wide range of drug delivery such as doxorubicin¹¹, cyclosporin¹², protein¹³, gene¹⁴ and so on. Selenocystine (SeC), a naturally occurring selenoamino acid, attracted much attention in the past years as it presented potential applications in pharmacology and cancer therapy^{15,16}. In our previous works, SeC was identified as a novel agent with higher antitumor activity than selenomethionine, Se-methyl-seleno-cysteine, selenite and selenate¹⁷ and was found to be less toxic to human normal cells. Despite this potency, the cancer selective mechanism of SeC remains elusive. SeC accumulated in cancer cells in a time-dependent manner, which resulted in time- and dose-dependent growth inhibition of cancer cells¹⁸. However, the poor stability and low solubility of SeC hindered its cell membrane permeabilization and the further development as an anticancer drug¹⁹. Based on the above consideration, the effective cellular

uptake of SeC must be taken into consideration when using as anticancer agents. Therefore, the development of cancer-targeted nanosystem to encapsulate SeC and further elucidation of the molecular mechanisms are urgently needed. In this study, by using natural products (CS), vitamin (folate acid, FA) and amino acids analogue (SeC), we fabricated a cancer-targeted nanosystem by encapsulating SeC into CS nanoparticles with folate decoration (FA-SeC-CSNPs) and evaluated its anti proliferative activity. The results showed that, this nanosystem could enter the cells through endocytosis and released SeC in lysosome under acidic environment. FA-SeC-CSNPs significantly inhibited the growth of HeLa human cervical cancer cells that overexpressed folate receptor through induction of apoptosis, with the involvement of PARP cleavage and caspase activation. Moreover, the nanoparticles also significantly suppressed the migration and invasion of HeLa cells in a dose-dependent manner. Furthermore, the intracellular nanosystem triggered the overproduction of ROS, which activated various downstream signaling pathways such as p53, AKT and MAPKs, to regulate the cell fate. Taken together, our results suggest that design and fabrication of food source nanomaterials could be a good way to achieve targeting drug delivery.

2 Materials and methods

Materials.

Selenocystine (SeC) was purchased from Fluka. Chitosan (CS), with a molecular weight of 60000 g/mol and the degree of deacetylation was 90.0%, was purchased from Beijing Ribio Biotech Co., LTD. folic acid (FA), glutaraldehyde (biological grade, 25%), 1-(3-Dimethylaminopropyl)-3-ethylcarbodiimide hydrochloride (EDC), 3-(4,5-dimethylthiazol-2-yl)-2,5 diphenyltetrazolium bromide (MTT) and pro-pidium iodide (PI) were purchased from Sigma-Aldrich Chemical Co. The water used for all experiments was ultrapure, supplied by a Milli-Q water purification system from Millipore. All of the solvents used were of HPLC grade. Dimethyl sulfoxide (DMSO) was purchased from Guangzhou Chemical Reagent Factory. Liquid paraffin and sorbitan sesquioleate were purchased from J&K Scientific. N-Hydroxysuccinimide (NHS) were purchased from Aladdin.

Fabrication of CSNPs.

A series of concentration solution (ranged from 15 mg/mL to 30 mg/mL) of CS in 5% aqueous acetic acid were dispersed in a mixture of 10 mL liquid paraffin containing 0.2 g of sorbitan sesquioleate in a 25 mL round-bottomed flask at room temperature. The finally volume ratio of water to oil ranged from 10:1 to 50:1. The dispersion was stirred using a stainless steel half-moon paddle stirrer at 2000 rpm for 30 min and 0.1 mL of glutaraldehyde saturated toluene were introduced into the flask and the stirring continued for 1 h. At the end, the CSNPs were filtered through a fritted disc, washed several

times with petroleum ether followed by methanol and finally with acetone. The CSNPs thus obtained were lyophilized and kept under refrigeration.

Fabrication of SeC-CSNPs.

Firstly, 10 mg SeC was added to 10 mL as-prepared CSNPs solution with EDC/NHS at room temperature and reacted 24 h. Then the mixture was dialyzed in distilled water for 24 h (MW cutoff = 6000-8000 kDa).

Fabrication of FA-SeC-CSNPs.

FA solution was treated with 400 mM EDC and 100 mM NHS for 15 min at room temperature with mild agitation to give the corresponding NHS-ester. SeC-CSNPs suspension in water (10 g/L) was added to the NHS-activated FA. FA of 2% weight compared with SeC-CSNPs concentration for 2 h at room temperature with gentle stirring. The resulting FA conjugated SeC-CSNPs, FA-SeC-CSNPs, were washed 3 times with water, lyophilized and kept under refrigeration. The conjugation content of folic acid in the nanoparticles were analyzed by spectrophotometry as previously described^{20, 21}.

Characterization of FA-SeC-CSNPs.

The obtained product of the FA-SeC-CSNPs was characterized by transmission electron microscopy (TEM), Zetasizer particle size analysis, fourier transform infrared spectra (FT-IR). The samples for TEM analysis were prepared by dispersing FA-SeC-CSNPs onto the holey carbon film on copper grids. The micrographs were obtained on Hitachi H-7650 system with acceleration voltage set at 80 kV. The Philips TECNAI 20 high-resolution transmission electron microscopy (HRTEM) worked at 400 kV. TEM-EDX analysis was carried out on the Philips TECNAI 20 high-resolution transmission electron microscopy and employed to examine the elemental composition of FA-SeC-CSNPs.

Determination of Se in the nanosystem and the cells.

Se concentration was determined by ICP-AES method²². The digested product was reconstituted to 10 mL with Milli-Q H₂O and used for ICP-AES analysis. Drug loading rate and encapsulation efficiency were calculated as follow. Drug loading rate (%) = drug (encapsulated)/mass of nanosystem×100%. Encapsulation efficiency (%)= drug (encapsulated)/drug (total)×100%.

Cell lines and cell culture.

Several human cancer cell lines, including A375 melanoma cells, HeLa cells, MCF-7 breast adenocarcinoma cells and L02, were purchased from American Type Culture Collection (ATCC, Manassas, VA). All cell lines were maintained in either RPMI-1640 or DMEM media, supplemented with fetal bovine serum (10%), penicillin (100 units/mL) and strep-

tomycin (50 units/mL) at 37 °C in CO₂ incubator (95% relative humidity, 5% CO₂).

MTT assay.

Cell viability was determined by measuring the ability of cells to transform MTT to a purple formazan dye²³. The cells were then incubated with samples at different concentrations for different periods of time.

Colony formation assay.

HeLa cells were centrifuged down after digestion, and seeded into 6-well plates at a density of 1500 cells/mL. 24 h after incubation, cells were treated with different concentrations of FA-SeC-CSNPs, FA-CSNPs, SeC-CSNPs, SeC and cisplatin for nine days, then the cells were fixed with methanol 10 min, washed with PBS twice, then stained with 0.5% crystal violet for 10 min.

Flow cytometric analysis.

The cell cycle distribution was analyzed by flow cytometry as previously described²⁴. Apoptotic cells with hypodiploid DNA content were measured by quantifying the sub-G1 peak in the cell cycle pattern. For each experiment, 10,000 events per sample were recorded.

Intracellular Localization of CSNPs.

The intracellular localization of CSNPs in HeLa cells was traced with 6-coumarin-labeled method as previously described²⁵. Briefly, the cells were cultured on cover glass in 6-well plates till 70% confluence were stained with 1 µg/mL Hoechst 33258 for 20 min. After washing with PBS twice, the cells were incubated with different concentrations of 6-coumarin-labeled CSNPs for various periods of time and examined under a fluorescence microscope (Nikon Eclipse 230 80i).

In vitro drug release of CSNPs.

Two copies of 10 mg of NPs were respectively suspended in 10 mL PBS solution at pH 5.3 and pH 7.4 with constantly shaking in dark tubes at 37°C. At specific intervals, a certain volume of buffer was taken out from tubes and same volume of fresh buffer was replaced. The collected buffer was centrifuged and the coumarin concentration was detected by modification of a literature method with fluorescence microplate reader²⁶.

Western blot analysis.

The effects of samples on the expression levels of proteins associated with different signaling pathways were examined by Western blot analysis²⁷.

Statistical Analysis.

All experiments were carried out at least in triplicate and results were expressed as mean ± S.D. Statistical analysis was performed using SPSS statistical program version 13 (SPSS Inc., Chicago, IL). Difference between two groups was analyzed by two-tailed Student's t-test. Difference with $P < 0.05$ (*) or $P < 0.01$ (**) was considered statistically significant. The difference between three or more groups was analyzed by one-way ANOVA multiple comparisons.

3 Results and Discussion

Fabrication and characterization of FA-SeC-CSNPs.

The preparation of CS nanoparticles was investigated by oil/water emulsification according to previously description with a tiny modification. Firstly, we have optimized the synthetic conditions of the nanoparticles to achieve small size distribution, cost-effective, higher drug-loading rate and encapsulation efficiency. This objective was achieved under the conditions of O:W=30:1 (Fig. S1) and CS concentration of 20 mg/mL (Fig. S2). Fig. 1A showed the proposed structure of FA-SeC-CSNPs. With the decoration of FA on SeC-CSNPs, the size of FA-SeC-CSNPs was found at about 200 nm (Fig. 1B). In addition to EDX spectrum, for individual nanoparticle, it collectively suggested that the nanoparticle possessed a mixture element with very high level of Se (Fig. 1C). Other minor signals of C and O probably originating from the CS were also observed. The average particles size of FA-SeC-CSNPs, investigated by a Zetasizer Nano-ZS particle analyzer, was found at 210 nm (Fig. S3A) which is consistent with TEM images. FA-SeC-CSNPs were further characterized by FT-IR to confirm the chemical binding of folate to the surface of CSNPs. Fig. S3B shows the FT-IR spectra of FA, SeC-CSNPs and FA-SeC-CSNPs, respectively. This peak 1 was attributed to C=O group and can be seen in the pure FA spectrum (at 1693 cm⁻¹). And the C–N stretching peak in the amide groups was found at 1385 cm⁻¹ (peak 2) and C–O in the ether groups was found at 1096 cm⁻¹ (peak 3) of SeC-CSNPs. Fig. S3C shows the FT-IR

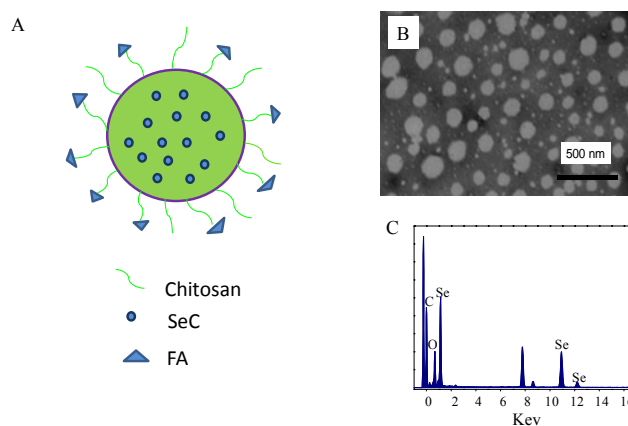


Fig. 1 Characterization of FA-SeC-CSNPs. (A) The diagrammatic figure of FA-SeC-CSNPs. (B) TEM images of FA-SeC-CSNPs with phosphotungstic acids as a negative stain. (C) EDX analysis.

spectra of CSNPs. The FT-IR spectra of FA-SeC-CSNPs resembled that of FA and SeC-CSNPs, giving clear evidence that the folate forms part of the nanocomposite. By using the ICP-AES analysis, drug loading rate (9.33%) and high encapsulation efficiency (51.13%) of SeC in the nanoparticles were observed (Table S1). The loading content of folic acid (FA) in the nanoparticles was found at 2.1%. FA-SeC-CSNPs were kept under refrigeration before the following biological evaluation.

In vitro anticancer activity of FA-SeC-CSNPs.

The antiproliferative activities of SeC, SeC-CSNPs, FA-CSNPs and FA-SeC-CSNPs were firstly screened against three human cancer cell lines and a normal cell line L02 liver cells by means of MTT assay, with cisplatin used as positive control. Fig. 2A shows the IC_{50} values of SeC, SeC-CSNPs, FA-CSNPs and FA-SeC-CSNPs after treatment for 72 h, with cisplatin used as positive control. FA-SeC-CSNPs exhibited broad-spectrum growth inhibition on MCF-7, A375 and HeLa cancer cell lines, with IC_{50} values ranging from 1.2 to 3.12 μ M which were significantly lower than that of L02 cells, indicating that the antiproliferative activities of SeC, FA-CSNPs, cisplatin and SeC-CSNPs toward cancer cells were much lower than that of FA-SeC-CSNPs on cancer cells. In addition, The results of colony formation assay obviously verify the stronger inhibitory effects of FA-SeC-CSNPs on HeLa cells (Fig. 2C). According to previous report, HeLa and MCF-7 cells were the folate receptor positive cells²⁸. These results suggest the feasibility of

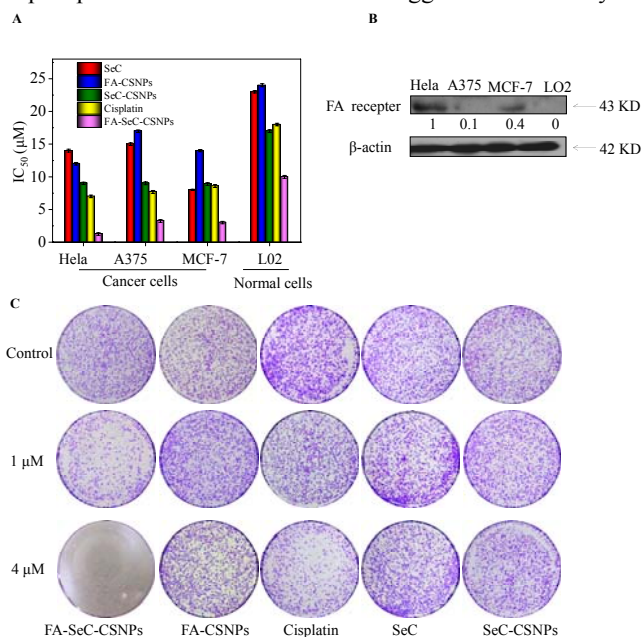


Fig. 2 (A) Cytotoxic effects of SeC, SeC-CSNPs, FA-CSNPs, cisplatin and FA-SeC-CSNPs on human cancer and normal cell lines. (B) Folate receptor (FAR) expression in HeLa, A375, MCF-7 and L02 cells. The expression level of FAR was determined by western blot analysis. (C) Effects of the nanoparticles on the colony formation activities of HeLa cells. The assay was performed in 6 well plates with cells exposed to SeC, FA-CSNPs, SeC-CSNPs, cisplatin and FA-SeC-CSNPs treatment for up to 10 days. Data are presented as mean \pm SD ($n = 3$).

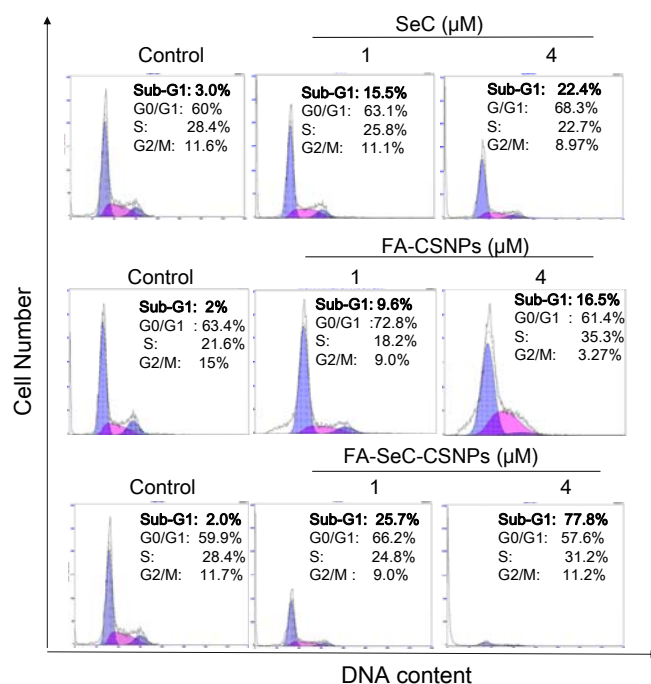


Fig. 3 Effects of SeC, FA-CSNPs and FA-SeC-CSNPs on the cell cycle distribution. Cells after treatment for 72 h were harvested and fixed with 70% ethanol before being stained with propidium iodide. Apoptotic cells with hypodiploid DNA content were measured by quantifying the Sub-G1 peak by flow cytometric analysis.

folate-guided selectivity between cancer and normal cells. FAR protein competing assay was used to further confirm this hypothesis. As shown in Fig. 2B, the expression levels of FAR in human cancer cells (HeLa and MCF-7) were significantly higher than L02 cells. These results are consistent with the appealing suggestion, namely that the selective antiproliferative activity of FA-SeC-CSNPs in human cancer cells, but not in normal cells, can be traced to FAR-mediated target. In order to elucidate the intracellular mechanisms for the enhancement of nanocarrier and SeC, also, we performed a DNA flow cytometric analysis to examine the change in cell cycle distribution. As reflected by the Sub-G1 cell populations, no significant apoptosis was observed in cells exposed to SeC and FA-CSNPs alone at 1 μ M (Fig. 3). Treatment of SeC and FA-CSNPs alone resulted in slight increase in the percentage of apoptotic cells from 3.0% (control) to 22.4% (4 μ M). However, significant increase in Sub-G1 cell populations was observed in cells treated with FA-SeC-CSNPs. For instance, the cells exposed to FA-SeC-CSNPs (4 μ M) displayed 77.8% of apoptosis. These results indicated that apoptosis is the major mode of cell death induced by combining treatment of SeC and cancer-targeting nanocarrier.

In Vitro Cellular Uptake and Localization of FA-coumarin-CSNPs.

To determine the *in vitro* drug release property of FA-SeC-CSNPs, nanoparticles containing a fluorescent dye 6-coumarin

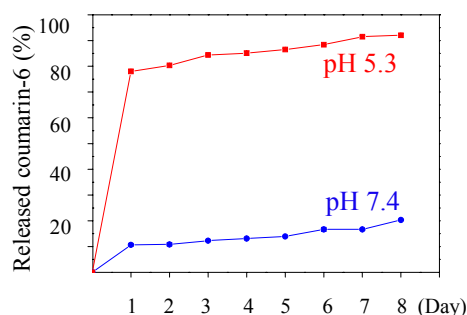


Fig. 4 Drug release of FA-SeC-CSNPs at different pH value solution. Data are presented as mean \pm SD ($n = 3$).

were prepared using similar procedure except that SeC was replaced by coumarin-6 (4 $\mu\text{g}/\text{mL}$) in the reaction system. The incorporated dye acts as a probe and offers a sensitive method to determine their intracellular uptake and localization. The *in vitro* drug release of coumarin from nanoparticles in PBS solution at pH 7.4 and in acetic acid solution at pH 5.3 was investigated to simulate the normal body blood and acidic environments. The results demonstrated that the release process at pH 7.4 was much slower than that at pH 5.3.

As shown in Fig. 4, the cumulative release of coumarin displayed a pH-dependent behavior. The main difference occurred after 24 h under two pH systems, with the release ratio reaching 78% for pH 5.3 and 10.6% for pH 7.4, respectively. Thereafter, the cumulative release of coumarin reached 92.1% at pH 5.3 and 20.3% at pH 7.4 after 8 days. This sustained release profile make the drug substance available over an extended period of time following ingestion, and could reduce the adverse side effects of free drugs, thus enhance its future application potential. Moreover, as the size swelling of CSNPs was slower in neutral than that of CSNPs in acid solution (Fig. 5), which indicate that the acid-stimulation responsive ability endowed the pH-responsive property of the nanosystem. Possibly, under neutral condition (pH=7.4), CS polymer was orderly aggregated due to the deprotonation of its amino groups, which hindered the release of SeC from nanoparticles. However, at pH 5.3, the behavior of protonated amino groups may lead to CS dissolution, which facilitated the release of SeC from FA-SeC-CSNPs.

Endocytosis is one of the most important entry mechanisms that influence the biodistribution for extracellular materials, particularly nanomaterials. Selective cellular uptake of therapeutic drugs remains a formidable obstacle for cancer therapy. Fluorescence imaging technique was also employed to gain more insights into the intracellular trafficking of FA-coumarin-CSNPs (green fluorescence). Two special fluorescent tracers, lyso-tracker (red) and DAPI (blue) were used to labeled lysosomes and nucleus. The results reveal that FA-coumarin-CSNPs moved across the cell membrane in 30 min, accumulated in lysosomes afterward, and finally dispersed in the whole cytoplasm, with bright, large fluorescence observed after 60 min (Fig. 6A). Meanwhile, no green fluorescence was

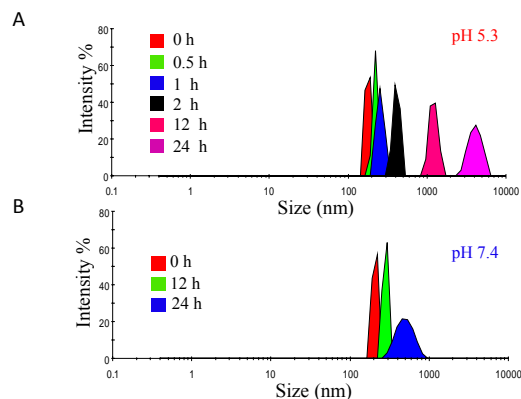


Fig. 5 Size distribution of FA-SeC-CSNPs at different pH value solution.

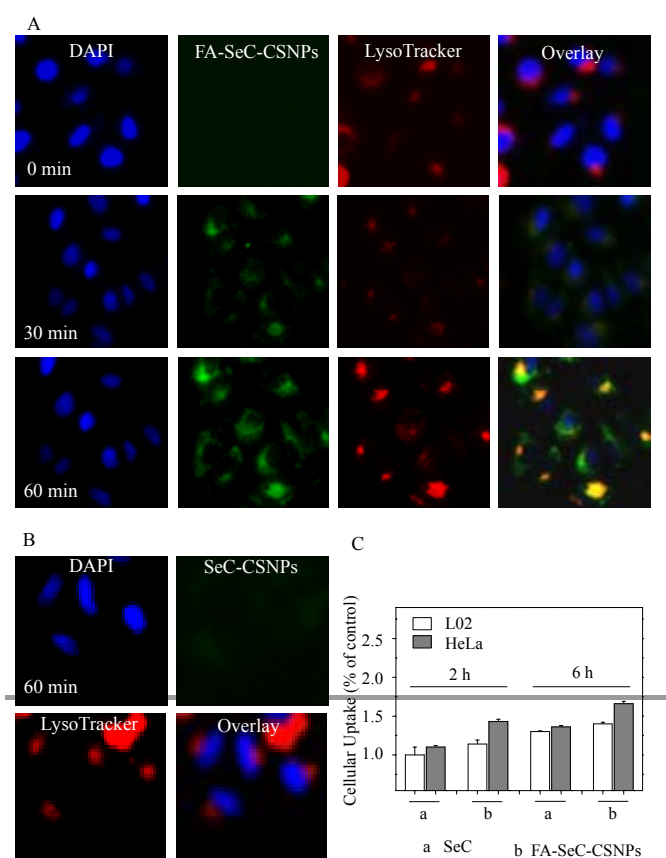


Fig. 6 Intracellular localization of FA-SeC-CSNPs (A), SeC-CSNPs (B) in HeLa cells and cellular uptake of Se concentrations in HeLa cells and L02 cells exposed to SeC and FA-SeC-CSNPs for 2 h or 6 h by ICP-AES method (C). Data are presented as mean \pm SD ($n = 3$).

observed in the cell nucleus during the whole process, suggesting that lysosome, but not nucleus, is the main cellular target of FA-coumarin-CSNPs. Interestingly, only very weak green fluorescence was observed in cells, indicating that it had few accumulation of coumarin-CSNPs (green fluorescence) without the decoration of folate in cells (Fig. 6B). It means that cellular uptake of coumarin-CSNPs was regulated by the folate decoration. To confirm this hypothesis, we examined the cellular uptake of SeC and FA-SeC-CSNPs in HeLa cells and

L02 cells treated for different time by using ICP-AES analysis. As shown in Fig. 6C, HeLa cells treatments with 20 μM FA-SeC-CSNPs for 6 h significantly increased the Se concentrations from 1.43 (% control, 2 h) to 1.66, which was significantly higher than that of SeC (1.36, 6 h). Interestingly, in L02 cells, it was found that treatments with FA-SeC-CSNPs increased the Se concentrations from 1.14 (2 h) to 1.4 (6 h), which was lower than those in HeLa cancer cells. Taken together, our results suggest that, comparing with SeC, the FA surface decoration contributed to the enhanced cellular uptake of FA-SeC-CSNPs in cancer cells.

Effects of FA-SeC-CSNPs on HeLa cells Migration and Invasion.

Studies were also conducted to compare the effects of SeC and FA-SeC-CSNPs on the HeLa cell migration and invasion. As shown in Fig. 7, the migration of HeLa cells decreased to 83%, 45% and 22% of control after treatment with SeC (2, 4 and 8 μM) for 24 h. Interestingly, greater inhibition on HeLa cell migration was observed in FA-SeC-CSNPs group. For instance, the migration index decreased to 39%, 10% and 1% of control after 24 h under the treatment at 1, 2 and 4 μM , respectively. In contrast, equal amount of the drug carrier, FA-CSNPs, induced the decrease of cell migration to 89%, 81% and 70% after 24 h treatment (Fig. S4). Moreover, transwell and Boyden assays were performed to investigate the effects of both treatments on invasion (Fig. 8). As expected, cell invasive ability decreased significantly in FA-SeC-CSNPs group, but lower effects were observed in cells exposed to SeC and FA-CSNPs groups (Fig. S5). Taken together, the results supported the hypothesis that FA-SeC-CSNPs inhibited cancer cell migration and invasion more effectively.

FA-SeC-CSNPs Induce Cell Apoptosis by generating of ROS.

Herein, we examined the activation and roles of ROS in the anticancer action of FA-SeC-CSNPs, FA-CSNPs and SeC at different concentration. Cells were exposed to different treatments at indicated conditions for different time, and then the intracellular ROS levels were analyzed by measuring the fluorescence intensity of an oxidation-sensitive fluorescein DCFH-DA. This fluorescence probe can penetrate the cell membrane freely and could be oxidized by ROS, resulting in strong green fluorescence. As shown in Fig. 9A, the cells treated with FA-SeC-CSNPs effectively triggered ROS generation in a time- and dose-dependent manner, which was much higher than those of SeC and FA-CSNPs groups. Especially, at the concentration of 5 μM , the ROS generation in FA-SeC-CSNPs group increased to 1.5 folds of control, while SeC and the empty vehicle alone only induced the ROS generation to 1.1 fold. These results were further confirmed by fluorescence microscopy. As shown in Fig. 9B, treatments of the cells with 5 μM FA-SeC-CSNPs led to the enhancement of cellular fluorescence in a time-dependent manner, with

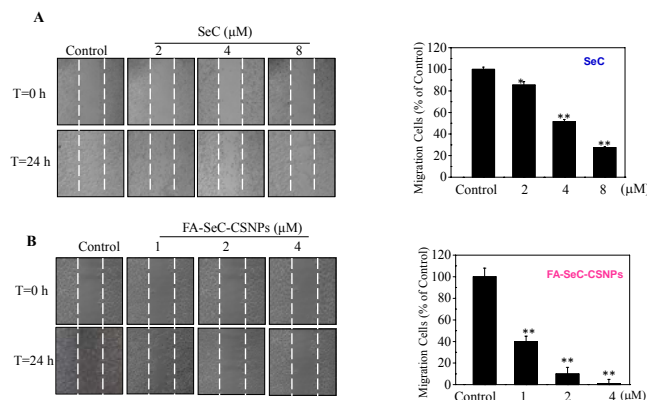


Fig. 7 Effects of SeC and FA-SeC-CSNPs on HeLa cells migration. Wound healing assay was performed 12 hours after plating. The total distance migrated by wounded cells was expressed as percentage of initial distance. Data are presented as mean \pm SD ($n = 3$). Difference with $P < 0.05$ (*) or $P < 0.01$ (**) was considered statistically significant comparing with the control group.

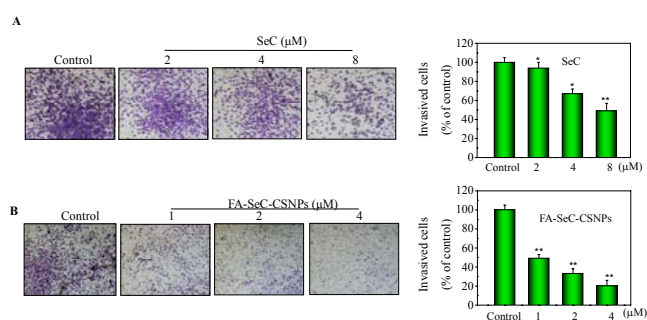


Fig. 8 Effects of SeC, and FA-SeC-CSNPs on HeLa cells invasion. The inhibition of cell invasion was measured by transwell and Boyden chamber assay. The number of cells was counted to calculate the average number of migrated cells. Data are presented as mean \pm SD ($n = 3$). Difference with $P < 0.05$ (*) or $P < 0.01$ (**) was considered statistically significant comparing with the control group.

maximum fluorescence observed after 80 min treatment. Taken together, these results suggest that FA-SeC-CSNPs trigger ROS overproduction in cancer cells through synergistic enhancement of SeC and the drug carrier FA-CSNPs. Western blotting was employed to confirm apoptosis in HeLa cells at the protein level. Several protein kinase pathways have been known to regulate cell proliferation and survival. AKT and MAPKs are major signal molecules closely related to the activation of p53 in most cell types. In the present study, as shown in Fig. 10A, FA-SeC-CSNPs obviously up-regulated the phosphorylation of p38 MAPK, but decreased the expression levels of phosphorylated Akt and ERK. Overproduction of ROS results in accumulation of oxidative products of DNA, such as DNA strand breaks (DSBs), DNA intra-strand adducts and DNA-protein crosslinks. In response to DSBs, ATM and ATR phosphorylate various downstream substrates, such as CHK1 and CHK2, H2AX and p53, to trigger cell apoptosis. In this study, we showed that, treatment of FA-SeC-CSNPs significantly elevated the phosphorylation of ATM and p53 (Fig. 10B), and enhanced the SeC cellular uptake and ROS accumulation. Moreover, significant DSBs inevitably caused the activation of p53

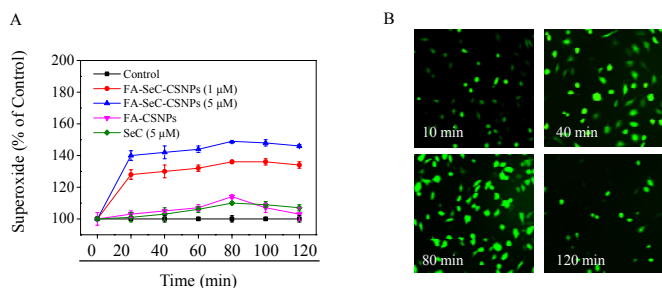


Fig. 9 The role of intracellular ROS generation in HeLa cell apoptosis induced by FA-SeC-CSNPs. (A) Cells were exposed to 1 and 5 μM FA-SeC-CSNPs, FA-CSNPs (equal amount to 5 μM FA-SeC-CSNPs) and 5 μM SeC for different times and the levels of the intracellular ROS were analyzed by measuring the fluorescence intensity of an oxidation-sensitive fluorescein DCFH-DA. (B) Fluorescence microscopy images of ROS generation in response to FA-SeC-CSNPs treatment for 10 min, 40 min, 80 min and 120 min, respectively, as detected by DCF-DA staining (magnification, 200 \times). Data are presented as mean \pm SD ($n = 3$).

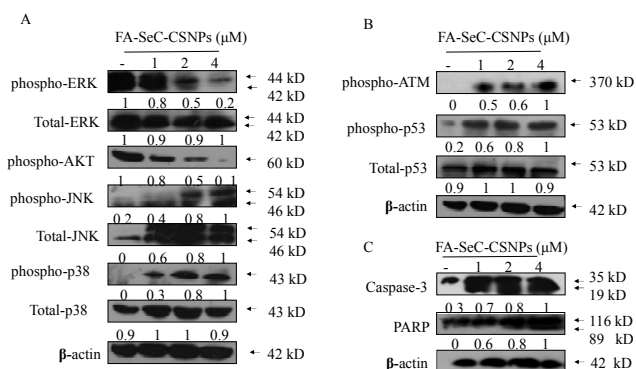


Fig. 10 Activation intracellular apoptotic signaling pathways by FA-SeC-CSNPs. (A) Effects of FA-SeC-CSNPs on Akt and MAPK signaling pathways. (B) DNA damage-mediated p53 activation. (C) Effects of FA-SeC-CSNPs on the expression levels of apoptosis-associated proteins PARP and Caspase-7 were analyzed by western blotting. Equal protein loading was confirmed by Western analysis of β -actin in the protein extracts.

pathway. Furthermore, it was shown that exposure of HeLa cells to the treatment of FA-SeC-CSNPs resulted in cleavage of caspase-3 (Fig. 10C), which subsequently induced the proteolytic cleavage of PARP, a protein serving as a biochemical hallmark of cells undergoing apoptosis.

4 Conclusions

In this study, by using natural polymer CS and FA, we fabricated a cancer-targeted nanodrug delivery system by encapsulating SeC into CS nanoparticles with FA surface decoration (FA-SeC-CSNPs), and evaluated its antiproliferative activities. The nanosystem entered the cells through endocytosis and released SeC under acidic environment into cytosol. FA-SeC-CSNPs significantly inhibited the growth of HeLa human cervical cancer cells that overexpressed folate receptor through induction of apoptosis with the involvement of PARP cleavage and caspase activation. Moreover, FA-SeC-CSNPs also significantly suppressed the migration and invasion of HeLa cells in a dose-dependent manner. Furthermore, the intracellular nanosystem triggered the overproduction of ROS,

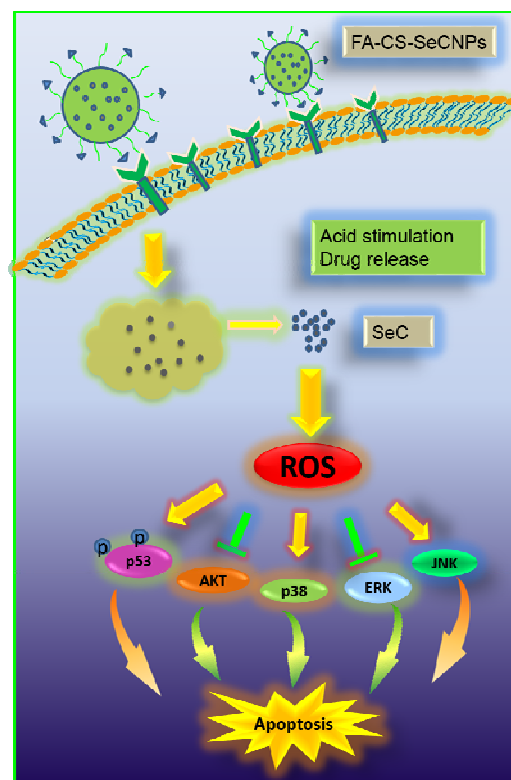


Fig. 11 Proposed signaling pathways of apoptosis induced by FA-SeC-CSNPs

which activated various downstream signaling pathways such as p53, AKT and MAPKs, to regulate the cell fate (Fig. 11). Taken together, this study demonstrate a strategy for rational design of cancer-targeted nanosystem loading selenocompounds to achieve selective cellular uptake and enhanced anticancer efficacy.

Acknowledgements

This work was supported by National High Technology Research and Development Program of China (863 Program, SS2014AA020538), Science Foundation for Distinguished Young Scholars of Guangdong Province, Natural Science Foundation of China and Guangdong Province, Program for New Century Excellent Talents in University, YangFan Innovative & Entrepreneurial Research Team Project, Research Fund for the Doctoral Program of Higher Education of China and China Postdoctoral Science Foundation.

Notes and references

The authors declare no competing financial interest.
 Department of Chemistry, Jinan University, Guangzhou 510632, China.
 # Authors contributed equally to the work.
 *To whom correspondence should be addressed.
 Tel: +86 20-85225962; Fax: +86 20 85221263.
 E-mail: tchentf@jnu.edu.cn.

† Electronic Supplementary Information (ESI) available.

1. A. H. El-Sagheer and T. Brown, *Acc. Chem. Res.*, 2012, **45**, 1258-1267.
2. E. Mamasheva, C. O'Donnell, A. Bandekar and S. Sofou, *Mol. Pharm.*, 2011, **8**, 2224-2232.
3. T. Shoji, E. Takatori, Y. Kaido, H. Omi, Y. Yokoyama, H. Mizunuma, M. Kaiho, T. Otsuki, T. Takano, N. Yaegashi, H. Nishiyama, K. Fujimori and T. Sugiyama, *Cancer Chemother. Pharmacol.*, 2014.
4. J. L. Markman, A. Rekechenetskiy, E. Holler and J. Y. Ljubimova, *Adv. Drug Deliv. Rev.*, 2013, **65**, 1866-1879.
5. L. Capuron, S. Geisler, K. Kurz, F. Leblhuber, B. Sperner-Unterweger and D. Fuchs, *Curr. Pharm. Des.*, 2014.
6. G. Kocic, L. Bjelakovic, B. Bjelakovic, T. Jevtoci-Stoimenov, D. Sokolovic, T. Cvetkovic, H. Kocic, S. Stojanovic, T. Langerholc and M. Jonovic, *J. Med. Food*, 2014.
7. S. Nishino, A. Itoh, H. Matsuoka, K. Maeda and S. Kamoshida, *Mol. Clin. Oncol.*, 2013, **1**, 661-667.
8. A. Pattani, V. B. Patravale, L. Panicker and P. D. Potdar, *Mol. Pharm.*, 2009, **6**, 345-352.
9. K. L. Kuo, W. C. Lin, I. L. Ho, H. C. Chang, P. Y. Lee, Y. T. Chung, J. T. Hsieh, Y. S. Pu, C. S. Shi and K. H. Huang, *PLoS One*, 2013, **8**, e68703.
10. X. Liu, X. Zhi, Y. Liu, B. Wu, Z. Sun and J. Shen, *J. Agric. Food Chem.*, 2012, **60**, 3471-3476.
11. K. A. Janes, M. P. Fresneau, A. Marazuela, A. Fabra and M. a. J. Alonso, *J. Controlled Release*, 2001, **73**, 255-267.
12. A. M. De Campos, A. Sánchez and M. a. J. Alonso, *Int. J. Pharm.*, 2001, **224**, 159-168.
13. Y. Xu and Y. Du, *Int. J. Pharm.*, 2003, **250**, 215-226.
14. B. Liu and L. Qian, *Guang Pu Xue Yu Guang Pu Fen Xi*, 1999, **19**, 610-612.
15. I. Cordero-Herrera, S. Cuello, L. Goya, Y. Madrid, L. Bravo, C. Camara and S. Ramos, *Food Chem. Toxicol.*, 2013, **59**, 554-563.
16. C. M. Weekley and H. H. Harris, *Chem. Soc. Rev.*, 2013, **42**, 8870-8894.
17. T. Chen and Y. S. Wong, *Int. J. Biochem. Cell Biol.*, 2009, **41**, 666-676.
18. T. Chen and Y. S. Wong, *J. Agric. Food Chem.*, 2008, **56**, 10574-10581.
19. J. Su, H. Lai, J. Chen, L. Li, Y. S. Wong, T. Chen and X. Li, *PLoS One*, 2013, **8**, e63502.
20. B. Yu, X. Li, W. Zheng, Y. Feng, Y.-S. Wong and T. Chen, *J. Mater. Chem. B*, 2014, **2**, 5409-5418.
21. S.-J. Yang, F.-H. Lin, K.-C. Tsai, M.-F. Wei, H.-M. Tsai, J.-M. Wong and M.-J. Shieh, *Bioconj. Chem.*, 2010, **21**, 679-689.
22. W. Liu, X. Li, Y.-S. Wong, W. Zheng, Y. Zhang, W. Cao and T. Chen, *ACS Nano*, 2012, **6**, 6578-6591.
23. M. Hao, A. M. Lowy, M. Kapoor, A. Deffie, G. Liu and G. Lozano, *J. Biol. Chem.*, 1996, **271**, 29380-29385.
24. S. Zheng, X. Li, Y. Zhang, Q. Xie, Y. S. Wong, W. Zheng and T. Chen, *Int. J. Nanomed.*, 2012, **7**, 3939-3949.
25. S. Zhang, H. Liu, H. Yu and G. J. Cooper, *Diabetes*, 2008, **57**, 348-356.
26. H. Tang, C. J. Murphy, B. Zhang, Y. Shen, E. A. Van Kirk, W. J. Murdoch and M. Radosz, *Biomaterials*, 2010, **31**, 7139-7149.
27. H. Wu, H. Zhuzhu, X. Li, Z. Li, W. Zheng, T. Chen, B. Yu and K. H. Wong, *J. Agric. Food Chem.*, 2013.
28. S. A. Kularatne, V. Deshmukh, M. Gymnopoulos, S. L. Biroc, J. Xia, S. Srinagesh, Y. Sun, N. Zou, M. Shimazu, J. Pinkstaff, S. Ensari, N. Knudsen, A. Manibusan, J. Y. Axup, C. H. Kim, V. V. Smider, T. Javahishvili and P. G. Schultz, *Angew. Chem. Int. Ed. Engl.*, 2013, **52**, 12101-12104.

Table of contents entry

A cancer-targeted chitosan nanocarrier has been rationally designed to enhance the selective cellular uptake and anticancer efficacy of selenocystine.

